



High aspect ratio MEMS capacitor for high frequency impedance matching applications

Yalcinkaya, Arda Deniz; Jensen, Søren; Hansen, Ole

Published in:

Proceedings of the 2003 10th IEEE International Conference on Electronics, Circuits and Systems, 2003. ICECS 2003.

Link to article, DOI:

[10.1109/ICECS.2003.1301937](https://doi.org/10.1109/ICECS.2003.1301937)

Publication date:

2003

Document Version

Publisher's PDF, also known as Version of record

[Link back to DTU Orbit](#)

Citation (APA):

Yalcinkaya, A. D., Jensen, S., & Hansen, O. (2003). High aspect ratio MEMS capacitor for high frequency impedance matching applications. In Proceedings of the 2003 10th IEEE International Conference on Electronics, Circuits and Systems, 2003. ICECS 2003. (Vol. 2). IEEE. DOI: 10.1109/ICECS.2003.1301937

General rights

Copyright and moral rights for the publications made accessible in the public portal are retained by the authors and/or other copyright owners and it is a condition of accessing publications that users recognise and abide by the legal requirements associated with these rights.

- Users may download and print one copy of any publication from the public portal for the purpose of private study or research.
- You may not further distribute the material or use it for any profit-making activity or commercial gain
- You may freely distribute the URL identifying the publication in the public portal

If you believe that this document breaches copyright please contact us providing details, and we will remove access to the work immediately and investigate your claim.

HIGH ASPECT RATIO MEMS CAPACITOR FOR HIGH FREQUENCY IMPEDANCE MATCHING APPLICATIONS

Arda Deniz Yalçınkaya, Søren Jensen and Ole Hansen

Mikroelektronik Centret, Ørsteds Plads, B-345-E, DTU
Technical University of Denmark, 2800, Kgs. Lyngby, Denmark

ABSTRACT

We present a micro electromechanical tunable capacitor with a low control voltage, a wide tuning range and adequate electrical quality factor. The device is fabricated in a single-crystalline silicon layer using deep reactive ion etching (DRIE) for obtaining high-aspect ratio (> 20) parallel comb-drive structures with vertical sidewalls. The process sequence for fabrication of the devices uses only one lithographic masking step and can be completed in a short time. The fabricated device was characterized with respect to electrical quality factor, tuning range, self-resonance frequency and transient response and it was found that the device is a suitable passive component to be used in impedance matching applications, band-pass filtering or voltage controlled oscillators in the Very High Frequency (VHF) and Ultra High Frequency (UHF) bands.

1. INTRODUCTION

Applications of tunable capacitors in integrated circuits spread in a wide segment. A tunable capacitor with a wide tuning range is a quite useful component for impedance matching purposes, as in the case of matching between the active interface circuitry (e.g. low-noise amplifier) and the passive components (e.g. 50Ω antenna) for maximum power transfer. Among the other applications are tunable filters [1], voltage controlled oscillators [2, 4] and resonators. As an example, high quality factor band pass filters are used in Intermediate Frequency (IF) blocks in heterodyne receivers, in the implementation of channel selecting filters with center frequencies ranging from 455 kHz to 254 MHz. Conventionally, RF blocks use electronic varactors implemented through diodes or transistors. Recently, micro electromechanical varactors have become a common interest of the RF community as an alternative technology to be used in the aforementioned applications [4, 5].

The quality factor of the MEMS capacitors is limited by the suspension spring which has to be compliant (or equivalently the beams have to be narrow and long) to enable low-voltage electrostatic actuation. This normally either calls for metallic structural layers [4] or deposition of thick metals on the signal path of the capacitor to reduce the series resistance [2, 3].

In this paper, we present an in-plane, high-aspect ratio tunable capacitor which can offer a wide tuning range with state of the art electronics compatible low actuation voltages. The tuning ratio was found to be 2:1 with 3 V of excitation voltage. Additionally, the capacitor settling time was measured as $200 \mu s$. Ambient air operation is enabled since the mechanical architecture of the system allows to obtain mechanical over-damped transient response. Characterizations at microwave frequencies showed that the

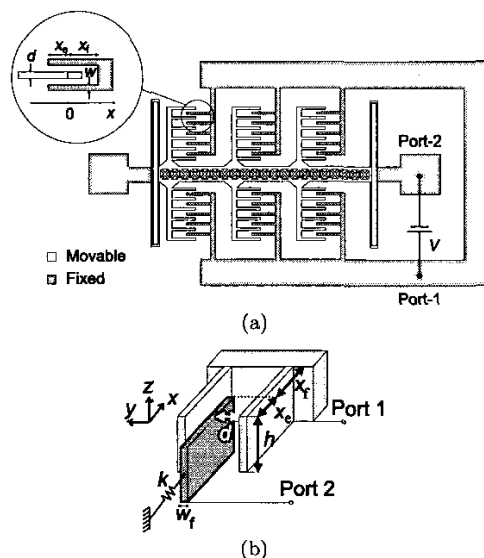


Figure 1. (a) Tunable capacitor schematic (b) Definitions for the geometries for comb fingers.

self-resonance frequency is above 4.08 GHz permitting high frequency operation without frequency range restrictions due to inductive effects.

2. DESIGN OF COMB-DRIVE VARACTORS

The tunable capacitors considered in this paper are comb structures, where the capacitance is realized through a number of interdigitated finger electrodes on a fixed and a movable part – the shuttle. The shuttle is suspended by a couple of folded beam springs with a low effective spring constant, k , for motion in the intended direction – the x -direction – and a high spring constant for motion in other directions. In Figure 1, a simplified sketch of one comb finger-pair with a schematic spring is shown. The fingers have the thickness w_f , the height h , and the length $x_e + x_f$, where x_e is the zero bias engagement of the fingers and x_f is the distance from the end of a finger to the bar connecting the unrelated fingers. The distance between neighboring fingers is d , which is in this analysis assumed independent on applied bias voltages due to the symmetry. N identical finger-pairs contribute an intended capacitance, C_I , which to a first order approximation, where fringe fields are ignored, can be obtained

as

$$C_I(x) = 2N\epsilon_0 \frac{h}{d}(x_e + x) = C_{I0} \left(1 + \frac{x}{x_e}\right), \quad (1)$$

where x is the displacement of the shuttle. Inherent to the design, however, is also an unwanted parasitic capacitance, C_P , between the end of the fingers and the finger connector bar, this capacitance limits the stroke length of the tunable capacitor. The parasitic capacitance for N fingers-pairs is approximately $C_P(x) = 2N\epsilon_0 \frac{h w_f}{x_f - x} = C_{P0}/(1 - \frac{x}{x_f})$.

The displacement, x , of the capacitor with an applied bias voltage is obtained by examining the potential energy, \mathcal{U} , of the system including the voltage source. The displacement is the solution to $\frac{\partial \mathcal{U}}{\partial x} = 0$, provided $\frac{\partial^2 \mathcal{U}}{\partial x^2} > 0$, otherwise the system is meta-stable and the fingers will snap to the finger connector bars. The total change in potential energy of the system is $\mathcal{U} = \frac{1}{2}kx^2 + \frac{1}{2}V^2(C_I + C_P) - V^2(C_I + C_0) = \frac{1}{2}kx^2 - \frac{1}{2}V^2(C_I + C_P)$. At small excursions, for a well designed device with $dw_f \ll x_f^2$, the displacement is approximately $x \simeq \frac{1}{2}V^2 2N\epsilon_0 \frac{h}{d} \frac{1}{k}$ and therefore the expected capacitance as a function of the applied bias is

$$C_I = C_{I0} \left(1 + V^2 \frac{N\epsilon_0 h}{kx_e d}\right) = C_{I0} \left(1 + V^2 \frac{C_{I0}}{2kx_e^2}\right). \quad (2)$$

The stability requirement $\frac{\partial^2 \mathcal{U}}{\partial x^2} > 0$, restricts the stable stroke (or travel) length; a simple calculation results in a maximum stable travel length of the shuttle, x_{\max} of

$$\frac{x_{\max}}{x_f} = 1 - \beta \left(\sqrt{\beta^3 + \beta^2} - \beta\right)^{-\frac{1}{3}} + \left(\sqrt{\beta^3 + \beta^2} - \beta\right)^{\frac{1}{3}} \quad (3)$$

where $\beta = \frac{dw_f}{x_f^2}$ is a design dependent parameter of the two capacitances C_I and C_P . At very small values of β , the maximum relative stroke length is close to 1, whereas at very high values of the parameter β , the maximum relative stroke length is limited to 1/3, as found in parallel plate actuators. The maximum stroke length limits the capacitor tuning range, since

$$\Delta C_{I\max} = C_I(x_{\max}) - C_{I0} = C_{I0} \frac{x_{\max}}{x_f} \frac{x_f}{x_e}. \quad (4)$$

In the present design, theoretical maximum obtainable capacitance change is $\Delta C_{I\max} \simeq 2.25 C_{I0}$.

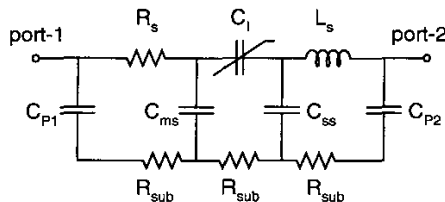


Figure 2. Equivalent circuit of the MEMS varactor.

Figure 2 shows the high-frequency equivalent of the device. In this schematic, the tunable capacitor is represented with C_I . R_s and L_s model the series (loss) resistor and inductive part of the interconnects, respectively. Two parasitic capacitors to the substrate (C_{P1} and C_{P2}) at each port are connected with handle wafer, which contributes a spreading resistance of R_{sub} .

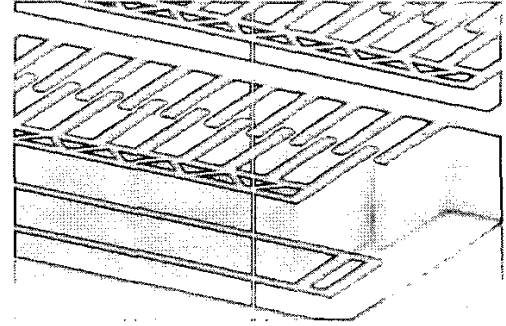


Figure 3. Overview SEM picture of the tunable capacitor. Inset: the detail of the comb-fingers.

3. FABRICATION

The tunable capacitor was fabricated in a simple single-mask process using dry deep reactive ion etching (DRIE)[6], followed by a wet isotropic release etch of a sacrificial silicon dioxide layer.

The starting material was a 4" (100) silicon-on-insulator substrate with a 50 μm thick device layer on top of a 1 μm thick oxide layer. The process sequence is illustrated in Figure 4.

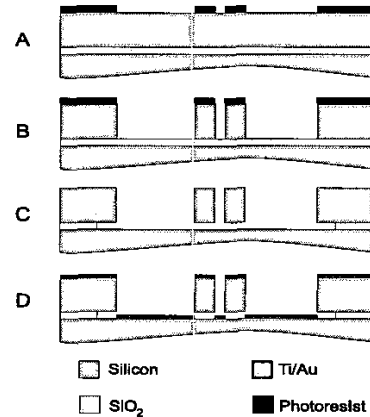


Figure 4. Tunable capacitor fabrication sequence. The silicon is etched using deep reactive ion etching (B). Afterwards, the narrow structure in the middle is released during the etch of the sacrificial silicon dioxide layer while the larger structures on the sides remain anchored (C). Finally, a Ti/Au layer is deposited on top of the device (D).

First, the geometry of the structures was patterned onto the substrate with 1.5 μm thick AZ5214 photoresist (Figure 4-A). Then, the masked substrate was then etched anisotropically in the DRIE tool until the buried oxide was reached. Due to the high aspect ratios of more than 1:20 and the narrow air gaps needed to obtain a high capacitance between the fingers, a novel etch recipe was developed (Figure 4-B). After the DRIE step, the remain-

ing photoresist was stripped in an O_2/N_2 plasma, and the narrow structures released in 40% hydrofluoric acid (Figure 4-C). Finally, a layer of 200 Å titanium and 5800 Å gold was evaporated on top of the devices to enhance the electrical quality factor (Figure 4-D).

For convenience, the process was carried out on a SOI substrate, which has a conducting handle wafer underneath the insulator layer. For application purposes, the process could be run on a handleless silicon-on-pyrex or silicon-on-fused-silica substrate without changes. This would eliminate parasitic substrate resistance (R_{sub}) and capacitances (C_{P1} and C_{P2}) and enhance the device performance. Such a process would lead a less well-defined air gap underneath the movable structure, but since most of the damping comes from the slide-film damping between the fingers, this would not deteriorate the device performance.

4. DEVICE CHARACTERIZATION AND APPLICATIONS

4.1. CV, Transient and RF characterizations

The tunable capacitors were characterized in air to extract the capacitance tuning curve and dynamic behavior. Open circuit calibration was performed before the measurements in order to compensate for the probe and pad capacitances [2]. The measured net device capacitance at 1 MHz is shown in Figure 5, revealing that the capacitance can be tuned between 1 pF (static capacitance) and 2 pF by varying the control voltage to 3.15 V where maximum deflection is obtained. Furthermore, in Figure 5, the expected capacitance from equation 2 using fabricated dimensions is overlaid on the experimental data, and is in good agreement with measurements. The experimental tuning range is 100%, mainly limited by the maximum excursion allowed by the spring anchors.

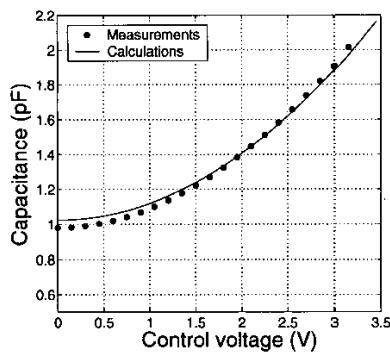


Figure 5. Capacitance-voltage tuning characteristic of the comb-driven tunable capacitors measured at 1 MHz. Numerical calculations with fabricated dimensions are in very good agreement with the experimental data.

The dynamic behavior of the mechanical system was explored at atmospheric pressure to extract the settling time using the C-t mode of the HP-4280A, with an external pulse biasing for fast measurements. The transient behavior was measured at 1 MHz employing a pulse voltage excitation of 1.2 V. The measurement was executed after the falling edge of the pulse to probe the recovery of the capacitance in time.

As can be seen from Figure 6, the capacitor settles to the final value in about 200 μs , with the desired over-damped response. The reason for the noise in the capacitance after 0.2 ms is the limited resolution of the HP-4280A in C-t mode. Contrary to other devices reported previously [1], the present device can safely be operated in ambient air without demanding a special package for the modification of medium viscosity or pressure.

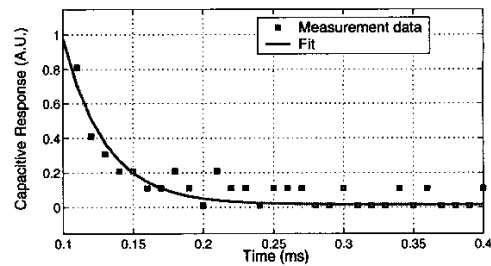


Figure 6. Transient response of the tunable capacitor. Measurements were performed after the falling edge of the excitation pulse (digitization of the capacitance value after 0.2 ms is due to the resolution of HP-4280A in C-t mode).

The microwave performance of the device was characterized through two-port scattering parameters from which the self-resonance behavior and electrical quality factor can be extracted. The measurement setup utilizes a Cascade probe station and ground-signal-ground configured probes with a standard pitch of 150 μm , connecting the device and the HP-8515A *s*-parameter test set through a micro-strip balanced coaxial cable. The HP-8510 network analyzer was then used for measurements at microwave frequencies. Having calibrated the probes for open circuit, short-circuit and 50 Ω load, the two-port *s*-parameters were measured in a frequency range of 45 MHz to 10 GHz. Figure 7 shows both simulated and measured s_{11} parameter in a Smith chart, where the frequency ranges from 45 MHz to 6 GHz.

With a measured device capacitance of 1 pF a quality factor of 100 at 100 MHz and roughly 10 at 1 GHz is obtained. Again, it can be observed from Figure 7 that, the device exhibits a self-resonance at 4.08 GHz.

4.2. Impedance Matching Applications

As an example usage of the tunable MEMS capacitor, the impedance matching circuit depicted in Figure 8 is designed. The circuit is a simple T-type impedance matching network for maximizing power transfer from a passive source resistance (R_S) to a complex load impedance ($Z_L = R_L + jX_L$) utilizing a grounded capacitance and two inductors (L_1, L_2) on the serial branch.

In order to emulate the complex load impedance (e.g. input impedance of a low noise amplifier), parallel combination of a resistor (200 Ω) and a capacitor (1 pF) is used. Figure 9 shows the magnitude of the voltage gain at the output node of the impedance matching network. As can be seen, from a 50 Ω source impedance, a near optimal power transfer (-3 dB) can be achieved in a rather wide frequency band (400 MHz - 800 MHz) by continuous tuning of the variable MEMS capacitor (2 pF to 1 pF) using a voltage range of 3.15 V to 0 V.

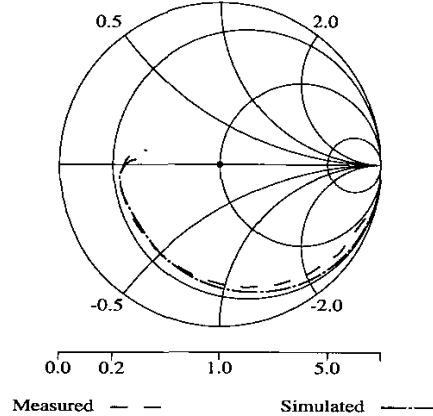


Figure 7. Simulated and measured reflection coefficient (s_{11}) of the MEMS tunable capacitor from 45 MHz to 10 GHz. Simulations are run using the equivalent circuit given in Figure 2, with measured values of C_I , R_s , C_{P1} and C_{P2} , and estimated values of R_{sub} and L_s .

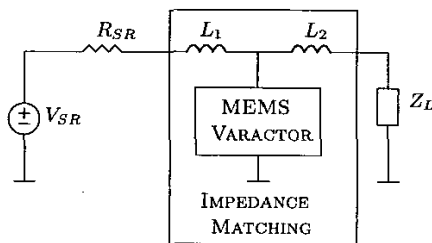


Figure 8. An example passive T-type network that utilizes MEMS tunable capacitor for matching a purely ohmic source impedance (R_{SR}) to an active complex impedance ($Z_L = R_L + jX_L$).

5. CONCLUSION

A high-aspect ratio tunable capacitor, that combines low-voltage actuation and wide tuning range, was successfully fabricated in a simple microfabrication process. By changing the standard recipe of the DRIE tool, an aspect ratio of 1:20 was obtained with vertical sidewalls. Performance characterizations have proved that the present device can be utilized to implement VHF and UHF tunable filters and impedance matching networks with electrical quality factors well above 100. A capacitance tuning ratio of 2:1 was achieved by changing the control voltage by only 3.15 V, enabling compatibility with the state of the art supply voltage range of integrated circuit technologies. The device has proven not to require any special treatment for a desired, fast transient response without any overshoot or oscillations, which was demonstrated by a pulse excitation measurement. High frequency measurements of the capacitor revealed a self-resonance of 4.08 GHz, which safely falls at least one order of magnitude above the intended frequency band of interest. As an example application, an RF impedance matching circuit is simulated which makes use of the MEMS tunable capacitor. Simulation results show that the wide tuning range of the capacitor enables

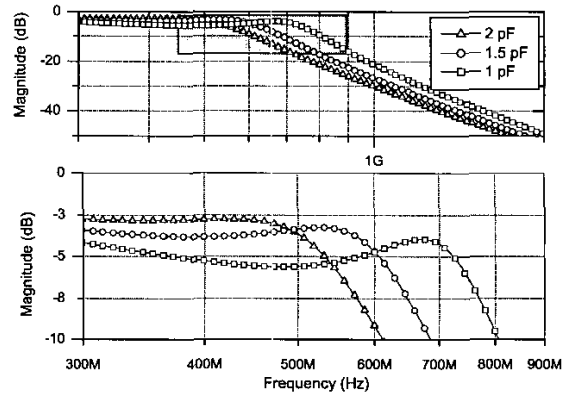


Figure 9. Simulation of the impedance matching network (Figure 8) using the tunable capacitor equivalent given in Figure 2. The source and the load impedances are chosen as $R_{SR} = 50 \Omega$ and $Z_L = 200 \Omega \parallel 1 \text{ pF}$, respectively. The inductors in the serial arms are 80 nH and 150 nH.

the matching in a wide frequency band. The current device offers improvements over solid-state varactors such as p-n junctions or metal-oxide-semiconductor capacitors, by expanding the design space for tunable VHF-UHF filters and impedance matching networks.

Acknowledgement

The authors wish to thank Mogens Pallisgaard of Electromagnetic Systems, Ørsted-DTU, Technical University of Denmark, for his kind assistance in s-parameter measurements.

6. REFERENCES

- [1] R.L. Borwick III, P.A. Stupar, J. DeNatale, R. Anderson, C.Tsai and K. Garrett "A high-Q, large tuning range, MEMS capacitor for RF filter systems" *Sensors and Actuators A*, **103**, pp. 33-41 (2003).
- [2] A. Dec and K. Suyama "Micromachined electromechanically tunable capacitors and their applications to RF IC's" *IEEE Trans. on Microwave Theory and Techniques*, **46**, pp. 2587-2596 (1998).
- [3] A.J. Gallant and D. Wood "Nickel electroplated widely tunable micromachined capacitor" *IEE Electronics Letters*, **38**, pp. 1392-1393 (2002).
- [4] D.J. Young and B.E. Boser "A micromachined capacitor for monolithic low-noise VCO", *Tech. Digest, Solid-State Sensor and Actuator Workshop*, pp.86-89, (1996).
- [5] J.J. Yao "RF MEMS from a device perspective", *J. Micromech. Microeng.*, **10**, R9-R-38, (2000).
- [6] A.M. Hynes, H. Ashraf, J.K. Bhardwaj, J. Hopkins, I. Johnston, and J.N. Shepherd, "Recent Advances in Silicon Etching for MEMS Using the ASE(TM) Process" *Sensors and Actuators A* **74**, pp. 13-17, (1999).